

Effects of hand configuration on muscle force coordination, co-contraction and concomitant intermuscular coupling during maximal isometric flexion of the fingers

Camille Charissou^{1,2,4} · David Amarantini² · Robin Baurès³ · Eric Berton¹ · Laurent Vigouroux¹

Received: 31 January 2017 / Accepted: 8 September 2017
© Springer-Verlag GmbH Germany 2017

Abstract

Purpose The mechanisms governing the control of musculoskeletal redundancy remain to be fully understood. The hand is highly redundant, and shows different functional role of extensors according to its configuration for a same functional task of finger flexion. Through intermuscular coherence analysis combined with hand musculoskeletal modelling during maximal isometric hand contractions, our aim was to better understand the neural mechanisms underlying

the control of muscle force coordination and agonist–antagonist co-contraction.

Methods Thirteen participants performed maximal isometric flexions of the fingers in two configurations: power grip (*Power*) and finger-pressing on a surface (*Press*). Hand kinematics and force/moment measurements were used as inputs in a musculoskeletal model of the hand to determine muscular tensions and co-contraction. EMG–EMG coherence analysis was performed between wrist and finger flexors and extensor muscle pairs in alpha, beta and gamma frequency bands.

Results Concomitantly with tailored muscle force coordination and increased co-contraction between *Press* and *Power* (mean difference: 48.08%; $p < 0.05$), our results showed muscle-pair-specific modulation of intermuscular coupling, characterized by pair-specific modulation of EMG–EMG coherence between *Power* and *Press* ($p < 0.05$), and a negative linear association between co-contraction and intermuscular coupling for the ECR/FCR agonist–antagonist muscle pair ($r = -0.65$; $p < 0.05$).

Conclusions This study brings new evidence that pair-specific modulation of EMG–EMG coherence is related to modulation of muscle force coordination during hand contractions. Our results highlight the functional importance of intermuscular coupling as a mechanism contributing to the control of muscle force synergies and agonist–antagonist co-contraction.

Communicated by Toshio Moritani.

Electronic supplementary material The online version of this article (doi:10.1007/s00421-017-3718-6) contains supplementary material, which is available to authorized users.

✉ Camille Charissou
camille.charissou@univ-amu.fr

David Amarantini
david.amarantini@inserm.fr

Robin Baurès
robin.baures@cnrs.fr

Eric Berton
eric.berton@univ-amu.fr

Laurent Vigouroux
laurent.vigouroux@univ-amu.fr

¹ CNRS, ISM UMR 7287, Aix-Marseille Université, Marseille, France

² ToNIC, Toulouse NeuroImaging Center, INSERM, UPS, Université de Toulouse, Toulouse, France

³ CerCo, Université de Toulouse, CNRS, UPS, Toulouse, France

⁴ Institut des Sciences du Mouvement-Etienne-Jules Marey, CP 910, 163 av. de Luminy, 13288 Marseille Cedex 9, France

Keywords Redundancy control · Wavelet-based intermuscular coherence · Hand modelling · Muscle tensions · Neural control

Abbreviations

ANCOVA Analysis of covariance
ANOVA Analysis of variance

CNS	Central nervous system
DoF	Degree of freedom
ECR	Extensor carpi radialis
EDC	Extensor digitorum communis
EMG	Electromyography
FCR	Flexor carpi radialis
FDS	Flexor digitorum superficialis
FE	Extrinsic finger extensor muscle group
FF	Extrinsic finger flexor muscle group
INT	Intrinsic muscles
N	Number of participants or sample size
SE	Standard error
WE	Extrinsic wrist extensor muscle group
WF	Extrinsic wrist flexor muscle group

Introduction

A fundamental feature of the musculoskeletal system is the high degree of redundancy, i.e., a greater number of muscles than articular degrees of freedom (DoF). As a consequence, muscle force combinations are infinite to achieve most isometric and dynamic motor actions, providing a large flexibility but making the control extremely complex (D'Avella et al. 2003). Understanding which mechanisms govern muscle force coordination and co-contraction of synergistic agonist and antagonist muscles is a central theme of research. As emphasized in recent studies (e.g., Hirashima and Oya 2016), a crucial question yet to be answered is how the central nervous system (CNS) solve such redundancy.

Regarding the control of muscle activation in voluntary contractions, it has been suggested that motoneurons of synergistic muscles share common corticospinal drives (Farmer et al. 2007) resulting in intermuscular coupling (Kattla and Lowery 2010). This coupling is translated by the oscillatory synchronicity of electromyographic (EMG) activity in synergistic muscle pairs, often called 'EMG–EMG coherence' (e.g., Danna-Dos-Santos et al. 2010). Previous studies reached a broad consensus that EMG–EMG coherence provides a comprehensive index of intermuscular coordination (Charissou et al. 2016; De Marchis et al. 2015). Through this approach, it was demonstrated that intermuscular coupling takes part to the regulation of muscle activities (Farmer et al. 2007; Siemionow et al. 2010) and the importance of such coupling was emphasized as a mechanism responsible for the maintenance of the neuromuscular performance (Charissou et al. 2016; Danna-Dos Santos et al. 2010). In addition, even though it is a highly debated issue (Farina et al. 2014), coherence between pairs of EMG signals would reflect common central drive to muscle pairs (Boonstra 2013; Farmer et al. 1998, 2007) and can thus be taken as a sensitive tool to explore common neural inputs implicated in the control of synergistic muscle activation during voluntary contractions

(Lee et al. 2014; Power et al. 2006; Wings et al. 2006). Associated with different neural processes, coordinated intermuscular coupling can arise from divergent descending oscillatory pathways (Heroux and Gandevia 2013; Nazarpour et al. 2012). Typically, the modulation of EMG–EMG coherence in the 'alpha' (α) frequency band impacts postural muscles and involuntary contractions (Boonstra et al. 2008; Kattla and Lowery 2010). There is every possibility that some of the α band coherence is of subcortical origin (Hansen et al. 2005; Poston et al. 2010) but it is also thought to be mediated by spinal sources (Budini et al. 2014; Norton and Gorassini 2006). Coherence in the 'beta' (β) frequency band has been linked with voluntary isometric contractions and is likely to reflect oscillatory drives from the corticospinal pathway (Chang et al. 2012; Gwin and Ferris 2012). Changes in the 'gamma' (γ) frequency band have been associated with efferent drives to muscles during very strong tonic contractions and cognitive processes, such as focused attention, resulting from cortical-originating signals (Mima et al. 2000). In light of previous studies on intermuscular synchronization (Poston et al. 2010; Wings et al. 2008), it may be proposed that, for a given task, modification of intermuscular coherence could represent a mechanism that contributes to the coordination of muscular forces according to the functional roles attributed to the muscles. Thus, the modulation of EMG–EMG coherence in the α , β and γ frequency bands could reflect mechanisms that solve synergistic muscle coordination—specifically reflecting a way of controlling agonist–antagonist co-contraction.

The hand and fingers are one of the most complex musculoskeletal systems and its fine control allows extremely diverse and complex movements. With 23 DoF and over 40 muscles, mostly polyarticular each mobilizing several DoF, the regulation of hand muscle coordination is extremely specific. The hand, thus, represents a reliable model that could bring further knowledge to current understanding of the mechanisms participating in the control of muscle force coordination between synergistic muscles, especially at the co-contraction level. Previous studies on hand musculoskeletal modelling demonstrated that muscle coordination patterns and force distribution are task specific (Valero-Cuevas et al. 2009). Especially, muscle force coordination and the functional role of the hand extensors can differ depending on whether hand contractions involve gripping objects or finger pressing on a plane surface, though in both configurations the same functional task is required which is to perform voluntary flexion of the fingers (Goislard de Monsabert et al. 2012; Snijders et al. 1987). During finger-pressing (see Fig. 1a), hand extensors are weakly mobilized, at a lower level than flexors, and are engaged in the hand joint postural stabilisation. Conversely, during power grip (see Fig. 1b), extensors are highly employed, approximately at the same

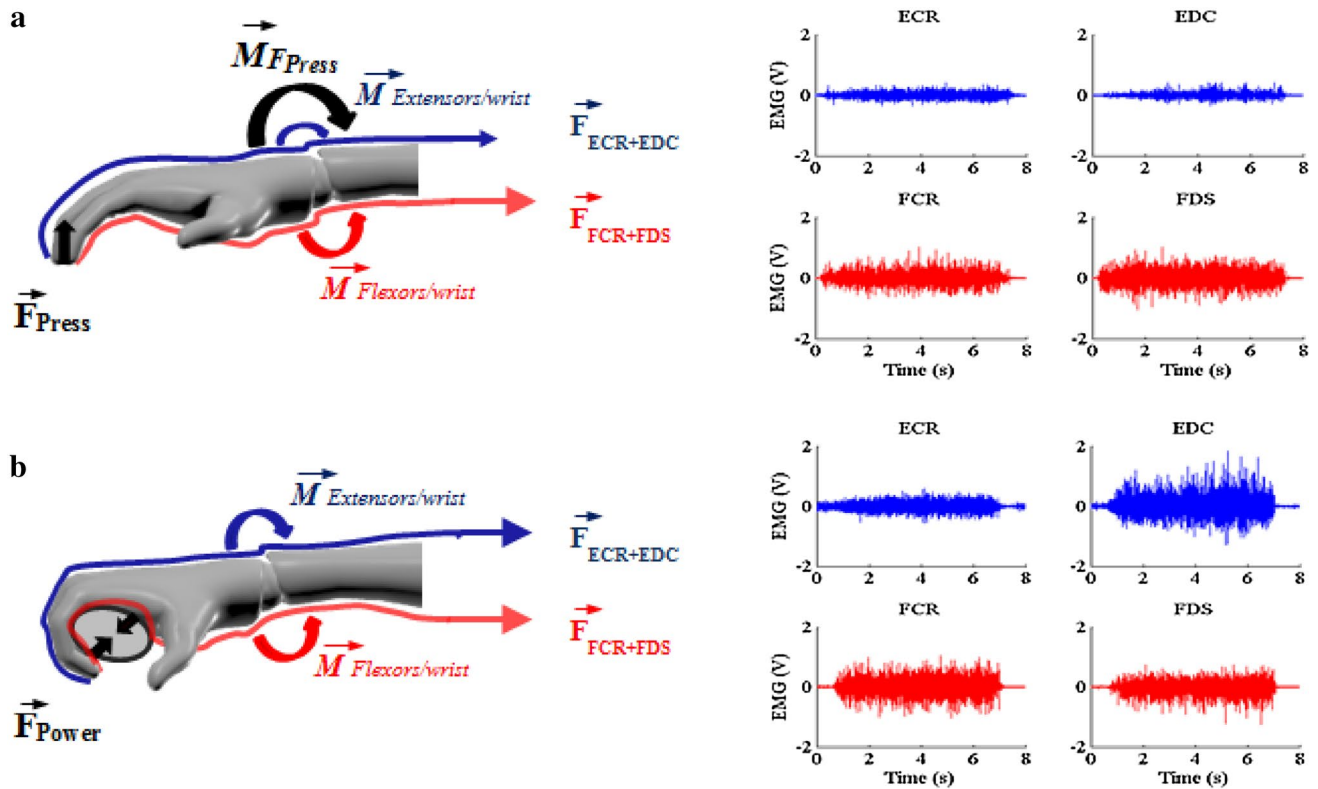


Fig. 1 Schematic representation of the two different configurations of finger force application in which participants performed maximal voluntary finger isometric flexion contractions: **a** “Finger pressing” (*Press*) and **b** “Power grip” (*Power*). F_{Power} and F_{Press} represent the force produced in the direction normal to the contact surface in *Power* and *Press*, respectively. $M_{Flexors/wrist}$, $M_{Extensors/wrist}$ and M_{FPress} represent the moments of force about the wrist joint. In each hand configuration, $F_{ECR+EDC}$ and $F_{FCR+FDS}$ represent the tension of extensor and flexor muscles, respectively. The right panels show high-pass-filtered (3 Hz, 4th-order zero-lag Butterworth) EMG activity of ECR,

EDC, FCR and FDS muscles in *Press* (upper panels) and in *Power* (lower panels). Note that with *Press*, the grip force generates a wrist moment (curved black arrow) leading to a low requirement of extensor mechanical action. With *Power*, no wrist moment is generated by the grip forces (black arrows) since the latter are balanced inside the hand-object mechanical system, this mechanical aspect, thus, explaining the higher wrist extensor muscle tensions required to balance the mechanical action of finger flexors at the wrist level. Such mechanical phenomenon leads to different muscle coordination which can be identified on the corresponding EMG patterns

level than flexors, and play a major functional role for system equilibrium. These observations suggest that muscle coordination strategies, co-contraction and consequently concomitant intermuscular coupling, differ between these two configurations of hand force application for a same functional task of finger flexion.

The aim of the present study was to better understand the neural mechanisms underlying the control of musculoskeletal redundancy. We harness the unique opportunity offered by hand contractions to clarify the functional significance of EMG–EMG coherence, reflecting tailored neural drive to hand muscles, in the control of muscle force coordination and in the regulation of co-contraction between synergistic agonist and antagonist muscles. The proposed approach thus combines hand/wrist musculoskeletal modelling (Goislard de Monsabert 2012)—used to quantify mechanical outcomes in terms of hand muscle

tensions and agonist–antagonist co-contraction—and time–frequency wavelet-based EMG–EMG coherence (Bigot et al. 2011; Charissou et al. 2016)—used to quantify intermuscular coupling in the alpha-, beta- and gamma range. Power grip and finger pressing were studied with the aim of changing the functional role of wrist and finger muscles for a same functional maximal isometric finger flexion. Based on previous research (Johnston et al. 2005; Poston et al. 2010), we hypothesized pair-specific differences in EMG–EMG coherence values between power grip and finger pressing, related to modulation of muscle force coordination. A correlation between intramuscular coherence, especially in the beta-range, and the level of agonist–antagonist co-contraction was expected. Such a linear association could reflect the functional importance of intermuscular coupling as a mechanism that contributes to the control of co-contraction.

Methods

Participants

Thirteen right-handed males (age: 24.8 ± 3.7 years; height: 176.8 ± 6.8 cm; weight: 74.2 ± 10.7 kg, hand length: 19.1 ± 1.2 cm; hand width: 8.7 ± 0.5 cm; mean \pm SD), free of known neuromuscular disorders or musculoskeletal hand injuries on their dominant side, were recruited in the study. All participants were physically active university students not involved in any specific training program. Written informed consent was obtained from all of them according to the Declaration of Helsinki. The study followed institutional ethics board guidelines for research on humans.

Protocol

Participants were seated in a comfortable position with their right arm placed on a rigid support so that the shoulder was flexed at 0° and abducted at 45° . The elbow was flexed at 90° and the forearm and wrist held in a neutral position. Participants were asked to perform maximal voluntary flexion contractions of the fingers in two different configurations of force application presented in random order (Fig. 1). During “power grip” contractions (*Power*), participants held a 3.5-cm custom-made hand dynamometer between the bottom of the palm of the hand and middle phalange of the fingers, excluding the thumb to avoid its influence on finger force coordination (Vigouroux et al. 2011). During “finger-pressing” contractions (*Press*), participants kept their hand horizontal and pressed vertically on the support with the index, major, ring and little fingers (Li et al. 1998). In each hand configuration, they performed five 6-s maximal contractions with strong verbal encouragements. They were allowed 2-min rest between contractions and 5-min rest between configurations to prevent muscle fatigue. Three participants were excluded from analysis because they failed to comply with the instruction to not overstretch the fingers in *Press*.

Recordings

The experimental setup was largely inspired by the work of Goislard de Monsabert et al. 2012. In brief:

- Forces and moments produced by the fingers were recorded by a 6-axis force/torque sensor (Nano25-E, ATI Industrial Automation, Apex, NC, USA) at 1 kHz. In *Press*, the force sensor was fixed on the support; in *Power* it was enclosed by two steel plates to apply the required mechanical effort.
- 3-D positions of the fingers, hand and forearm segments and of the dynamometer (in *Power*) or the surface (in *Press*) were recorded at 125 Hz by an 8-camera system

(MX T40, Vicon, Oxford, UK) with 33 spherical reflective markers of 6-mm diameter (Suppl. Figure 1a).

- After suitable skin preparation (Hermens et al. 2000), muscle activities were collected at 2 kHz using a surface EMG system (MP150; Biopac Systems Inc., Goleta, CA, USA) with Ag-AgCl 11-mm bipolar electrodes (2 cm spacing). *Flexor digitorum superficialis* (FDS), *flexor carpi radialis* (FCR), *extensor digitorum communis* (EDC), and *extensor carpi radialis* (ECR) were taken to represent finger flexors (FF), wrist flexors (WF), finger extensors (FE) and wrist extensors (WE), respectively. Using the recommendations in Vigouroux et al. (2015), pairs of surface electrodes were placed along the direction of muscle fascicles of right FDS, FCR, EDC and ECR muscles (Suppl. Figure 1b) from anatomical description, palpation and a series of functional tests including finger and wrist flexion and extension contractions. Moreover, the quality of the electrical signal was inspected through a visual feedback using the software AcqKnowledge (BIOPAC, Systems Inc., Goleta, CA, USA), before the beginning of voluntary isometric contractions to assess correct EMG sensor location in the desired target muscle.

Data processing

All computations were performed using MATLAB (Mathworks, Natick, MA, USA).

Maximal net force After calibration matrix application of the force/torque sensor and low-pass filtering (10 Hz, fourth-order, zero-lag Butterworth), maximal net force was calculated as mean normal force computed on the 0.5-s time interval of interest of highest force production.

Muscular tensions A musculoskeletal model of the entire hand including wrist and fingers (Goislard de Monsabert et al. 2012) was used to estimate muscular forces over the time period of interest in the two configurations of force application. This model considered bones as rigid bodies articulated around 16 articulations with 23 DoF and mobilized by 42 muscles. The muscle moment arms of muscle tendons across each joint were estimated from the finger joint angles computed using 3D hand kinematics and the data of Chao et al. (1989) and Lemay and Crago (1999). The underdetermined set of static moment equilibrium equations stating that the external force moments are counterbalanced by the muscle force moments at each DoF was solved using nonlinear constrained optimization to determine the muscle tensions which minimize the following muscle stress criterion:

$$\min \sum_m \left(\frac{t_m}{PCSA_m} \right)^4$$

where t_m and $PCSA_m$ are respectively the muscle tensions and the physiological cross-sectional area of muscle m .

For the nine participants for whom the optimization process converged to a global minimum of the cost function in less than 1000 iterations, tension of finger and wrist flexor muscle group was then obtained by summing FF and WF tensions, while that of the finger and wrist extensor muscle group was quantified by summing FE and WE tensions, (Vigouroux et al. 2015). Noteworthy is that INT was not considered in the analysis as EMG was not collected from these muscles and they do not cross the wrist joint. Finally, muscle group tensions were used to compute co-contraction between finger and wrist flexors and extensors according to the expression given by Falconer and Winter (1985).

EMG–EMG coherence Given strong a priori evidence from the literature that *Press* and *Power* functionally differ by the specific role of the wrist extensors (Snijders et al. 1987), this work focused on ECR/FCR, ECR/FDS and ECR/EDC muscle pairs. For each muscle pair, intermuscular coherence analysis was performed using the approach described by Charissou et al. (2016; see ‘Intermuscular interactions’ in “Methods” and Online Appendix A), which:

- takes advantage of time–frequency analysis to account for how the oscillatory patterns of EMG change with time;
- presents the crucial advantage to assess coherence with values corresponding to a truly significant level of dependence between the EMG time series, particularly when the number of trials is small (Bigot et al. 2011).

First, EMG–EMG coherence was calculated in the time–frequency domain using the *WavCrossSpec* software (Bigot et al. 2011; available for download at: http://www.math.u-bordeaux1.fr/~jbigot/Site/Software_files/WavCrossSpec.zip). In *WavCrossSpec*, the parameter ‘nvoice’ (i.e., the scale resolution of the wavelet), ‘J1’ (i.e., the number of scales used in the wavelet analysis) and ‘wavenumber’ (i.e., the Morlet mother wavelet parameter) optimally set respectively to 7, 50 and 10 based on the processing of simulated data, to provide a satisfactory compromise between time and frequency resolution for the identification of oscillatory activity on the $[0.32 \times 10^{-2}; 0.23; 79.97]$ Hz frequency range. To meet the theoretical and practical recommendations of previous studies (e.g., Bigot et al. 2011; McClelland et al. 2014), magnitude-squared coherence (Fig. 2, fourth row) was computed from unrectified high-pass filtered (3 Hz, 4th-order zero-lag Butterworth) EMG time series (Fig. 2, first row) as follows:

$$R_{EMG1/EMG2}^2(\omega, u) = \frac{\left| S_{EMG1/EMG2}(\omega, u) \right|^2}{\left(S_{EMG1}(\omega, u) S_{EMG2}(\omega, u) \right)'}$$

where $S_{EMG1/EMG2}(\omega, u)$ is the wavelet cross-spectrum between the two EMG time series at frequency ω and time u (Fig. 2, third row); $S_{EMG1}(\omega, u)$ and $S_{EMG2}(\omega, u)$ are wavelet auto-spectra of EMG time series at frequency ω and time u . (Fig. 2, second row). Refer to Bigot et al. (2011) for detailed equations.

Then, EMG–EMG coherence was quantified in ‘alpha’ (α), ‘beta’ (β) and ‘gamma’ (γ) frequency bands. In agreement with previous intermuscular coherence studies (Danna Dos Santos et al. 2010; Kattla and Lowery 2010), boundaries were respectively set as follows: α , 8–12 Hz; β , 15–35 Hz; γ , 35–60 Hz. In each frequency band, EMG–EMG coherence value was calculated as the volume under magnitude-squared coherence values in the time window of interest where the correlation between the EMG time series was detected significant on the wavelet cross-spectrum (Fig. 2, fifth row).

Statistics

All kinetic variables met normality (Shapiro–Wilk test, $\alpha = 0.05$) and homogeneity of variance (Levene’s test, all $p > 0.05$) assumptions. Student’s *t*-tests were used to assess between-*Configuration* effects (*Press* vs. *Power*) on maximal net force ($N = 10$), predicted muscular tensions and co-contraction ($N = 9$). A 2 *Configuration* (*Press* vs. *Power*) \times 2 *Muscle Function* (*Flexors* vs. *Extensors*) repeated measures ANOVA was performed on muscle group tensions ($N = 9$).

For each muscle pair and frequency band, an ANCOVA was first performed on EMG–EMG coherence ($N = 10$) with *Configuration* as a within-participant factor and maximal net force as a co-variable, to check if EMG–EMG coherence was influenced by the *Configuration* while controlling for the exerted net force. Indeed, it is yet unclear how exerted net force may (1) affect EMG–EMG coherence (Farina et al. 2014; Heroux and Gandevia 2013; Semmler et al. 2003; Witte et al. 2007), and (2) have a different influence on EMG–EMG coherence depending on the *Configuration*. Importantly, this analysis failed to show any significant interaction between *Configuration* and the maximal net force (all $p > 0.05$), showing a lack of correlation between EMG–EMG coherence and maximal net force for each *Configuration*. However, EMG–EMG coherence values failed to meet both normality and homogeneity of variance assumptions. As used in other studies in the presence of skewed distribution (e.g., Vrána et al. 2005), permutation tests with bootstrapping technique (Efron and Tibshirani 1993) with 10,000 replications were, thus, conducted for each muscle pair and frequency band to test between-*Configuration* differences on EMG–EMG coherence irrespective of the maximal net force. A significant effect of *Configuration* was declared significant if the observed difference between *Power* and *Press* was outside the 95% confidence interval of the newly built 10,000 mean difference distributions under the null hypothesis.

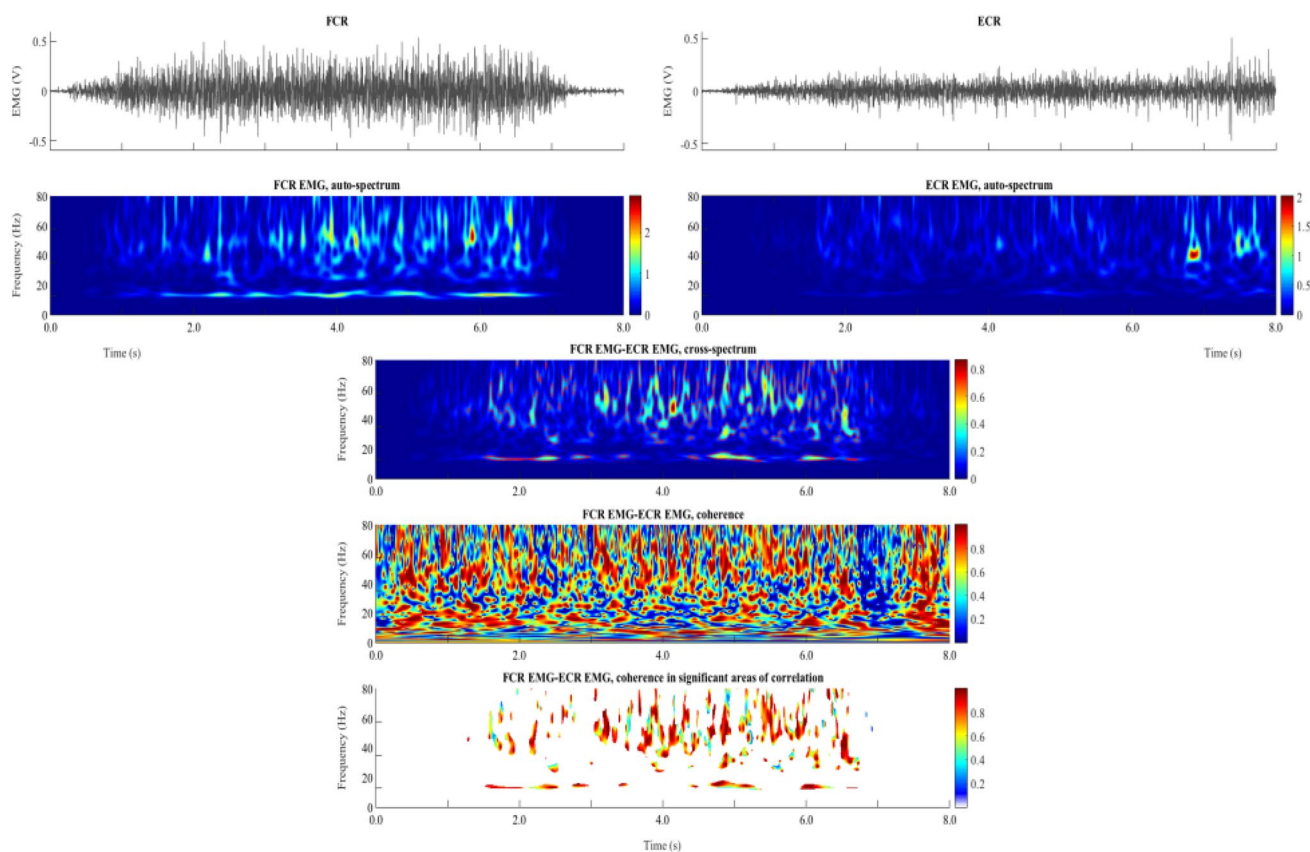


Fig. 2 Illustration of the different steps involved in the calculation of time–frequency wavelet-based EMG–EMG coherence (muscle pair: ECR/FCR; configuration: *Press*). First row: mean EMG signals from FCR (left) and ECR (right) muscles. Second row: wavelet auto-spectra of EMG time series from FCR (left) and ECR muscles (right). Third row: wavelet cross-spectrum between the two EMG time series; the red contours identify the areas in the time–frequency plane where the correlation between the EMG signals is significant. Fourth row:

wavelet magnitude-squared coherence between the two EMG time series. Fifth row: wavelet magnitude-squared coherence between the two EMG time series where the correlation between the EMG signals is significant. In each frequency band (α : 8–12 Hz; β : 15–35 Hz; γ : 35–60 Hz), EMG–EMG coherence value was defined as the volume under magnitude-squared coherence values in the 0.5-s time window of interest where the correlation between the EMG time series was detected significant on the wavelet cross-spectrum

Finally, Pearson’s correlations were tested between co-contraction and EMG–EMG coherence for each muscle pair and frequency band ($N=9$).

Data are reported as mean with 95% CI within the text and Figs. 3 and 4. The level of significance was set at $p < 0.05$ for all tests.

Results

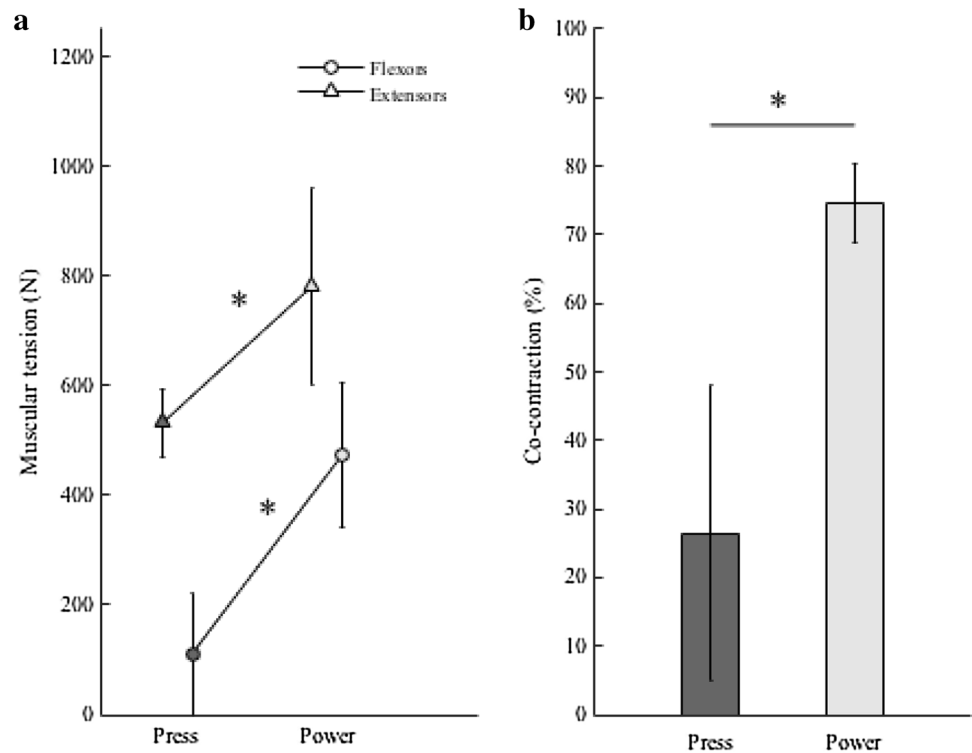
Maximal net force and muscular tensions

Statistical analysis revealed greater maximal net force in *Power* than in *Press* [232.14 N, 95% CI (188.59:275.68) vs. 76.13 N, 95% CI (66.55:85.70); $t_8 = 7.59$, $p < 0.05$], in association with significant differences in all estimated

muscular tensions (all $t_8 > 2.13$, $p < 0.05$): between *Press* and *Power* the tensions developed by WE, FE and FF increased in mean respectively by $\times 1.40$, $\times 0.92$ and $\times 3.04$ the corresponding difference of maximal net force, whereas WF tension decreased in mean by $\times 1.44$. These differences resulted in significantly increased tensions developed by the finger and wrist flexors and extensors between *Press* and *Power* ($F_{1,32} = 29.34$, $p < 0.05$; Fig. 3a), with a significant main *Muscle Function* effect ($F_{1,32} = 41.61$, $p < 0.05$) but no significant interaction between *Configuration* and *Muscle Function* ($F_{1,32} = 0.98$, $p > 0.05$).

As a consequence, co-contraction between finger and wrist flexors and extensors was significantly higher in *Power* than in *Press* [mean difference = 48.08%, 95% CI (24.57:71.60); $t_8 = 4.62$, $p < 0.05$; Fig. 3b].

Fig. 3 ($N=9$) **a** Tensions of finger and wrist flexors and extensors during maximal isometric contractions in *Press* and *Power*. **b** Corresponding co-contraction levels in *Press* and *Power*. Asterisk: indicates a significant *Configuration* effect



EMG–EMG coherence

Figure 4a show typical profiles of the normal force exerted by the fingers and typical time–frequency maps of EMG–EMG coherence between ECR and FCR muscles in *Press* (left) and *Power* (right).

A first important qualitative result was that the detection of significant areas of intermuscular interactions in the time–frequency plane differed depending on the muscle pair (i.e., ECR/FCR, ECR/FDS or ECR/EDC) and the *Configuration* level (i.e., *Power* or *Press*). For example, significant areas of correlation between EMG time series were detected for all participants in all muscles pairs in *Press* and in *Power* in the γ (35–60 Hz) frequency band. A similar finding was observed in terms of detection for, e.g., ECR/EDC muscle pair in *Press* in the β (15–35 Hz) frequency band, whereas, on the contrary, no significant area of correlation between EMG time-series were found for, e.g., ECR/FCR muscle pair in *Power* in the α (8–12 Hz) frequency band.

Noteworthy is that the proposed ANCOVA pre-analysis performed on EMG–EMG coherence (see “**Statistics**” section) showed that the lack of correlation between EMG–EMG coherence and maximal net force was true for all *Configuration* levels, whatever the frequency band. These findings allow one to compare EMG–EMG coherence results between *Power* and *Press* irrespective of the exerted maximal net force.

Statistical analysis revealed that β EMG–EMG coherence was significantly lower in *Power* than in *Press* for both ECR/FCR [mean difference = 0.191, 95% CI (0.05:0.241); $p < 0.05$] and ECR/EDC [mean difference = 0.494, 95% CI (–0.047:0.941); $p < 0.05$] muscle pairs, with no significant difference for ECR/FDS (Fig. 4b, middle). In the gamma-range (γ), statistical analysis showed lower EMG–EMG coherence in *Power* than in *Press* for ECR/EDC muscle pair [mean difference = 1.003, 95% CI (0.439:1.567); $p < 0.05$], with no significant difference for both ECR/FCR and ECR/FDS (Fig. 4b, right). Permutation tests disclosed significant difference of α EMG–EMG coherence between *Press* and *Power* for all muscle pairs (all $p > 0.05$) (Fig. 4b, left).

Correlations between co-contraction and EMG–EMG coherence

Pearson’s correlation analysis between co-contraction and EMG–EMG coherence showed significant negative correlation between levels of co-contraction and β EMG–EMG coherence for ECR/FCR muscle pair [$r = -0.65$, 95% CI (–0.86:–0.26); $t_{16} = 3.42$, $p = 0.003$] and ECR/EDC muscle pair [$r = -0.47$, 95% CI (–0.77:–0.01); $t_{16} = 2.15$, $p = 0.04$]. For both muscle pairs (see Fig. 5 for ECR/FCR), the lower was β EMG–EMG coherence, the higher was agonist–antagonist co-contraction between finger and wrist flexors and extensors. For all other frequency bands and muscles

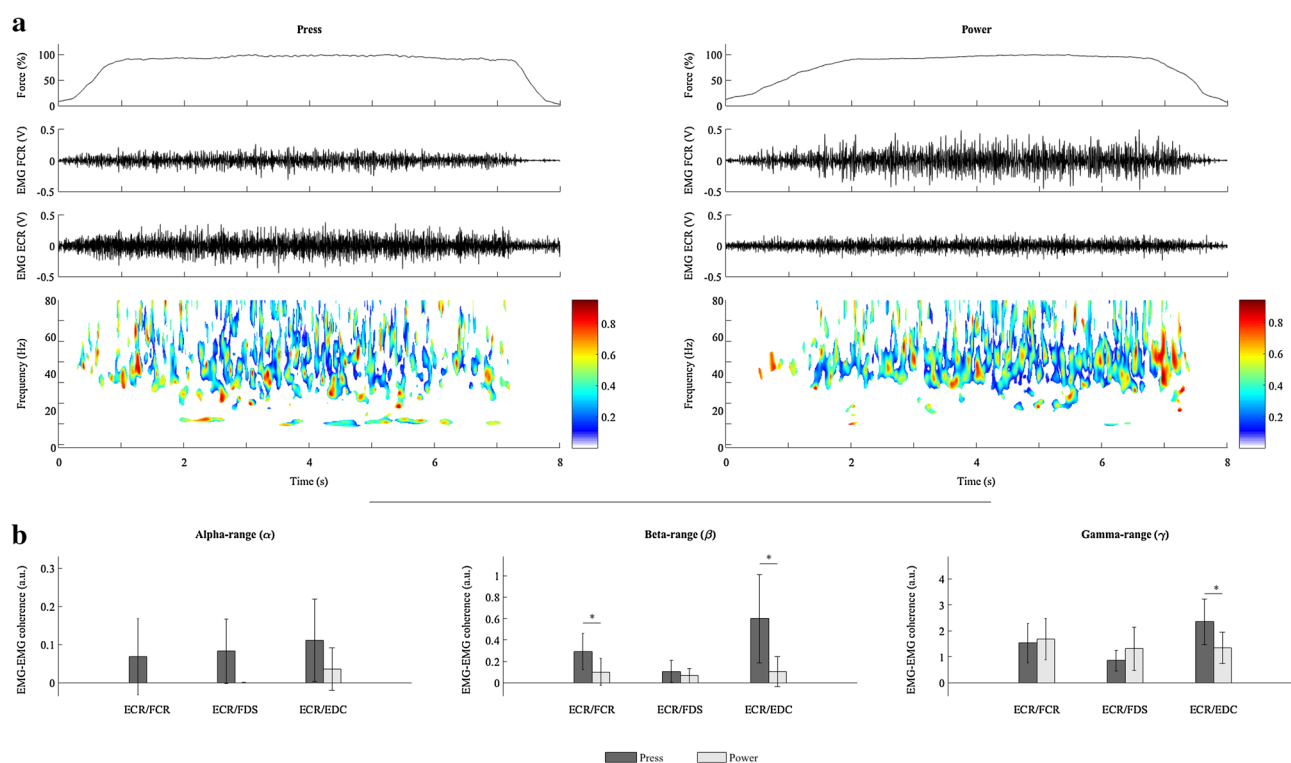


Fig. 4 **a** Typical net force (first row), EMG signal from ECR and FCR (second and third rows, respectively), and maps of EMG–EMG coherence between ECR and FCR muscles where intermuscular interactions were significant on the wavelet cross-spectrum (forth row) in *Press* (left panels) and *Power* (right panels) for a representative participant. **b** EMG–EMG coherence values in the alpha-range

(8–12 Hz, α ; left column), the beta-range (15–35 Hz, β ; middle column) and the gamma-range (35–60 Hz, γ ; right column) for ECR/FCR, ECR/FDS and ECR/EDC muscle pairs during maximal voluntary isometric flexion contraction of the fingers in *Press* and *Power* ($N=10$). Asterisk: indicates a significant *Configuration* effect

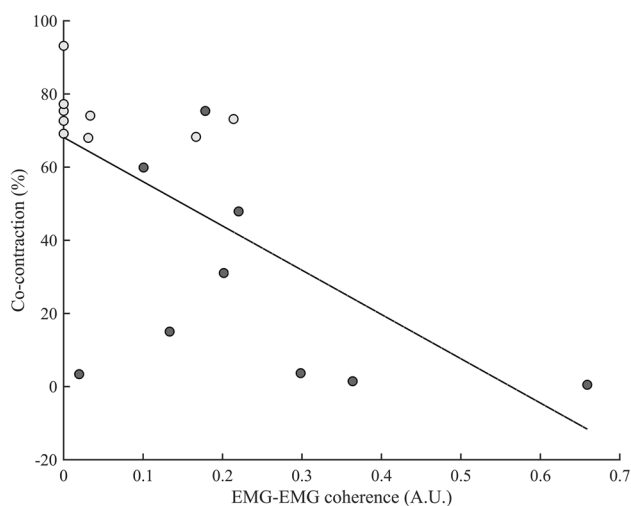


Fig. 5 Correlation between co-contraction of finger and wrist flexors and extensors and β (15–35 Hz) EMG–EMG coherence for ECR/FCR muscle pair ($N=9$). The light grey and dark grey dots represent observations in *Power* and in *Press*, respectively; the black line shows the best fit linear regression. The Pearson product-moment correlation coefficient is -0.65 [95% CI = $(-0.86;-0.26)$], with significant negative linear association between co-contraction and EMG–EMG coherence ($p=0.003$)

pairs (including EDC/FCR, EDC/FDS and FCR/FDS, not presented here) the analysis did not reveal any significant correlation between co-contraction and EMG–EMG coherence (all $t_{16} < 0.89$, $p > 0.05$).

Discussion

Based on an original approach, which combines for the first time musculoskeletal biomechanical modelling and intermuscular coherence analysis, this study compares muscular tensions, co-contraction and intermuscular coupling between finger and wrist flexors and extensors during two different configurations of maximal finger force application. Our key results demonstrated first, that the modulation of muscle force coordination and intermuscular coherence are strongly related to the task constraints, and second, that a linear association exists between agonist–antagonist co-contraction and beta-range intermuscular coupling for the primary agonist–antagonist muscle pair.

Maximal net force and muscular tensions

As expected, *Power* and *Press* differed greatly in muscle force coordination. Greater maximum net force was obtained in *Power* than in *Press* in association with (1) higher tensions developed by WE, FE and FF, and (2) lower tension developed by WF. These results showed that *Configuration*-related changes in maximal net force were not accompanied by a trivial or a proportional modulation of muscle tensions. Each muscle tension demonstrated a specific pattern of change between *Press* and *Power*, suggesting that muscle-synergy patterns used to perform maximal voluntary flexion contractions of the fingers are highly dependent on the configuration of finger force application. During *Press*, the extensors were weakly solicited and coupled with a classical role of joint stabilisation, resulting in low-level of co-contraction. Conversely, during *Power*, the extensors were highly mobilized to serve the functional role of system equilibrium, culminating in high level of co-contraction. These results were comparable to those reported for both configurations in the literature (Goislard de Monsabert et al. 2012) and demonstrated task-related changes in muscle force coordination (Nazarpour et al. 2012; Valero-Cuevas et al. 2009). Consequently, co-contraction level was different between the two configurations. The higher co-contraction observed in *Power* has been explained previously (Snijders et al. 1987) by specific mechanical configuration in which the contribution of extensors was needed to equilibrate unintended flexion moments caused by finger flexors at the wrist joint level. Our data thus demonstrated that muscle coordination patterns differed according to the configuration of finger force application, although the functional demand to exert maximal voluntary flexion was similar between *Power* and *Press*.

Together with the possibility to discuss between-*Configuration* differences on EMG–EMG coherence irrespective of the maximal net force, these findings confirm that the proposed comparison between *Power* and *Press* is relevant to investigate the modulation of EMG–EMG coherence according to different muscle coordination and functional role of muscles for a similar given task.

EMG–EMG coherence

Concomitantly with the above changes in muscle forces, our results revealed significant differences in the magnitude of EMG–EMG coherence, with different modulation patterns in both the frequency band (α , β or γ) and the muscle pair (ECR/FCR, ECR/FDS or ECR/EDC) according to the configuration (*Press* vs. *Power*). One cannot exclude the possibility that a part of EMG–EMG coherence may result from cross-talk artifacts inherent to surface EMG recordings, especially among the forearm muscles (Kong et al.

2010). Nevertheless, our experimental design devoted particular attention to EMG sensor placement (see “*Recordings*” section) and the same electrode placement was maintained during all the experiment. We thus are confident in the fact that cross-talk artifacts or electrode placement (Keenan et al. 2011) cannot explain the differences observed on EMG–EMG coherence between the two *Configurations*.

The statistical pre-test revealed that the difference observed between *Press* and *Power* in the absolute maximal net force did not influence the magnitude of EMG–EMG coherence. This result contributes to the open debate on the influence of net-exerted muscle force/torque on the strength of intermuscular coupling (Farina et al. 2014; Heroux and Gandevia 2013). In agreement with Poston et al. (2010), this finding provides direct support for a net force-independent modulation of intermuscular coherence during voluntary maximal flexion contraction of the wrist and fingers muscles. It suggests an involvement of force-independent mechanisms constraining the concurrent activation of multiple hand muscles according to the configuration of finger force application. Importantly for the purpose of the present study, the observed lack of significant correlation between EMG–EMG coherence and maximal net force for each *Configuration* allows discussing for differences in EMG–EMG coherence values depending only on the *Configuration*.

Beta-range (β) intermuscular coupling

The main findings of our study concern beta-range (β) intermuscular coupling. In the β (15–35 Hz) frequency band, significant EMG–EMG coherence was detected for all muscle pairs in both configurations. This first result is consistent with the identification of β intermuscular synchronization between synergistic muscles (Boonstra et al. 2008; Poston et al. 2010). In addition, the magnitude of EMG–EMG coherence was different between *Power* and *Press* only for ECR/EDC and ECR/FCR. For these two muscle pairs, the strength of beta-range intermuscular coupling was lower in *Power* than in *Press*, while no significant difference was found for ECR/FDS. This finding is in line with Winges et al. (2008) indicating that the modulation of β EMG–EMG coherence is muscle pair specific. In view of the results obtained from hand modelling, it is particularly relevant to note that the lower strength of intermuscular coupling observed in *Power* than in *Press* was concomitant with the increased tension developed by wrist extensors identified with the musculoskeletal model outputs. Our results are thus consistent with the hypothesis that beta-range intermuscular coupling is a mechanism that may take part in the regulation of muscle force coordination (Charissou et al. 2016; De Marchis et al. 2015). Moreover, we extend the evidence provided by Winges et al. (2006) that β EMG–EMG coherence

differs according to muscle functional role determined by task constraints.

Furthermore, our study is the first to the best of our knowledge, to show a direct link between agonist–antagonist co-contraction and β EMG–EMG coherence. Our results from hand modelling indeed showed that *Configuration*-related changes in muscle tensions led to greater agonist–antagonist co-contraction in *Power* than in *Press*. Interestingly, correlation analysis revealed significant negative correlations between the level of co-contraction and beta-range intermuscular coupling for ECR/FCR and ECR/EDC, that is for the two muscle pairs specifically associated with a significant effect of *Configuration* on β EMG–EMG coherence. Especially, with a r value of -0.65 ($p=0.003$) the correlation between the level co-contraction and EMG–EMG coherence for ECR/FCR muscle pair indicates linear association between co-contraction and intramuscular coupling for the primary agonist–antagonist muscle pair. For ECR/EDC muscle pair, although the correlation is significant ($p=0.04$), it becomes more difficult with a weak r value of -0.45 to find support for a linear relationship between co-contraction and intermuscular coupling. In line with Pizzamiglio et al. (2017), who recently suggested that ~ 40 – 100 Hz intermuscular coupling could take part in regulating the co-contraction of arm muscles, these novel findings suggest that the modulation of β EMG–EMG coherence may reflect a mechanism contributing to muscle pair-specific regulation of co-contraction between synergistic agonist and antagonist muscles. Our results thus highlight that muscle pair-specific modulation of intermuscular coupling could take part in the “tuning of muscle activations” (von Tscharner et al. 2011) and in the mechanisms underlying the regulation of agonist–antagonist co-contraction. Even if the conclusions should be considered in regards to the reliability and the limitations of coherence analysis between electrophysiological signals (e.g., Farina et al. 2014), β -band coherence is generally considered to be of cortical origin and it is likely “that the primary motor cortex is involved in the generation of EMG–EMG coherence between hand muscles in the β -band during grip tasks” (Lee et al. 2014). In this view, our findings strengthen the idea formulated by Poston et al. (2010) that the relative contribution of spinal and supraspinal mechanisms is modulated according to task constraints and beyond muscle contribution and functional role. Furthermore, our results on tailored modulation of beta-range intermuscular coupling between *Press* and *Power* provides additional arguments sustaining a muscle pair-specific distribution of common neural inputs to the hand muscles (Johnston et al. 2005) during maximal voluntary isometric flexion contraction of the fingers. These results support the view that central

mechanisms are directly involved in the regulation of agonist–antagonist muscle co-contraction (Dal Maso et al. 2012; Mullany et al. 2002). Our study thus provides new evidence that muscle pair-specific beta-range intermuscular coupling would take part in the regulation of muscle redundancy around hand joints, especially at the level of agonist–antagonist co-contraction.

Alpha-range (α) intermuscular coupling

In the α (8–12 Hz) frequency band, statistical analysis showed no significant effect of *Configuration* on intermuscular coupling, whatever the studied muscle pair. This finding is not consistent with previous studies that showed that hand postural function was associated with modulation of α EMG–EMG (Poston et al. 2010). However, from a more qualitative point of view, our results showed that the presence of EMG–EMG coherence in the α (8–12 Hz) frequency band was different according to both the muscle pair and the hand configuration. Especially, an absence of α EMG–EMG coherence was identified for all subjects only in *Power* and only for the ECR/FCR muscle pair. This finding was concomitant with the modulation of the level of co-contraction between *Press* and *Power*, associated with the postural functional role of ECR during *Press*. One could thus suggest that α EMG–EMG coherence was specifically required between synergistic agonist and antagonist muscles acting around the wrist when the extensors were specifically involved as joint stabilisers. Our results may thus support the importance of alpha-range intermuscular coupling between agonist and antagonist muscles as a key mechanism in the control of joint stabilisation. Even if previous studies have reported that α -band coherence may be mediated by spinal sources (Budini et al. 2014; Norton and Gorassini 2006), further work is needed to investigate the involvement of spinal mechanisms in the regulation of agonist–antagonist co-contraction when the task needs particular heeding requisites for joint stability.

Gamma-range (γ) intermuscular coupling

In the γ (35–60 Hz) frequency band, significant intermuscular coherence was found for all studied muscle pairs in both *Press* and *Power* configurations. This finding is consistent with the relation previously established between γ EMG–EMG coherence and strong contractions (Gwin and Ferris 2012). However, significant modulation of γ EMG–EMG coherence was found for ECR/EDC muscle pair only, with higher strength of intermuscular coherence in *Press* than in *Power*. Although it is difficult to arrive at a definitive conclusion with regards to the literature, we can suggest that the observed pair-specific modulation of gamma-range (γ) intermuscular coherence between

synergistic antagonist muscles may reflect the implication of efferent drives involved in very strong tonic contractions and of cognitive processes, such as focused attention (Mima et al. 2000). Brown et al. (1998) suggested that gamma-range oscillations may reflect binding of functionally associated cortical elements. Thus, non-intuitively in view that power grip was seen only in humans and highly-developed monkeys (Marzke et al. 2015), our findings may suggest that attentional resources and complex integration of sensory information are used during hand contractions in both configurations, with greater involvement during finger pressing.

Conclusion

The present work harnesses the opportunity offered by hand contractions and combined musculoskeletal and time–frequency coherence analysis to better understand the neural mechanisms underlying the control of muscle force coordination and co-contraction between agonist and antagonist synergistic muscles. Although further studies are needed to test whether our conclusions can be extended to other muscles than those acting around finger and wrist joints selected in the present study, our findings emphasized the functional importance of intermuscular coupling as a mechanism that could take part in the control of muscle force synergies and agonist–antagonist co-contraction. These findings contribute to a better fundamental understanding of neural hand motor control mechanisms, which could help in the development of diagnostic procedures and clinical rehabilitation (Boonstra 2013).

Compliance with ethical standards

Conflict of interest The authors declare that there are no conflicts of interest.

References

- Bigot J, Longcamp M, Dal Maso F, Amarantini D (2011) A new statistical test based on the wavelet cross-spectrum to detect time–frequency dependence between nonstationary signals: application to the analysis of cortico-muscular interactions. *Neuroimage* 55:1504–1518
- Boonstra TW (2013) The potential of corticomuscular and intermuscular coherence for research on human motor control. *Front Hum Neurosci* 7:855
- Boonstra TW, Daffertshofer A, van Ditzhuijzen JC, van den Heuvel MR, Hofman C, Willigenburg NW, Beek PJ (2008) Fatigue-related changes in motor-unit synchronization of quadriceps muscles within and across legs. *J Electromyogr Kinesiol* 18:717–731
- Brown P, Salenius S, Rothwell JC, Hari R (1998) Cortical correlate of the Piper rhythm in humans. *J Neurophysiol* 80:2911–2917
- Budini F, Lowery M, Durbaba R, De Vito G (2014) Effect of mental fatigue on induced tremor in human knee extensors. *J Electromyogr Kinesiol* 24:412–418
- Chang YJ, Chou CC, Chan HL, Hsu MJ, Yeh MY, Fang CY, Chuang YF, Wei SH, Lien HY (2012) Increases of quadriceps intermuscular cross-correlation and coherence during exhausting stepping exercise. *Sensors* 26:16353–16367
- Chao EY, An KN, Cooney WP III, Linscheid RL (1989) *Biomechanics of the hand: a basic research study*. World Scientific, Singapore
- Charissou C, Vigouroux L, Berton E, Amarantini D (2016) Fatigue- and training-related changes in ‘beta’ intermuscular interactions between agonist muscles. *J Electromyogr Kinesiol* 27:52–59
- d’Avella A, Saltiel P, Bizzi E (2003) Combinations of muscle synergies in the construction of a natural motor behavior. *Nat Neurosci* 6:300–308
- Dal Maso F, Longcamp M, Amarantini D (2012) Training-related decrease in antagonist muscles activation is associated with increased motor cortex activation: evidence of central mechanisms for control of antagonist muscles. *Exp Brain Res* 220:287–95
- Danna-Dos-Santos A, Poston B, Jesunathadas M, Bobich LR, Hamm TM, Santello M (2010) Influence of fatigue on hand muscle coordination and EMG–EMG coherence during three-digit grasping. *J Neurophysiol* 104:3576–3587
- De Marchis C, Severini G, Margherita Castronovo A, Schmid M, Conforto S (2015) Intermuscular coherence contributions in synergistic muscles during pedaling. *Exp Brain Res* 233:1907–1919
- Efron B, Tibshirani RJ (1993) *An introduction to the bootstrap*. Chapman & Hall
- Falconer K, Winter DA (1985) Quantitative assessment of co-contraction at the ankle joint in walking. *Electromyogr Clin Neurophysiol* 25:135–149
- Farina D, Negro F, Dideriksen JL (2014) The effective neural drive to muscles is the common synaptic input to motor neurons. *J Physiol* 592:3427–3441
- Farmer SF (1998) Rhythmicity, synchronization and binding in human and primate motor systems. *J Physiol* 1:3–14
- Farmer SF, Gibbs J, Halliday DM, Harrison LM, James LM, Mayston MJ, Stephens JA (2007) Changes in EMG coherence between long and short thumb abductor muscles during human development. *J Physiol* 579:389–402
- Goislard de Monsabert B, Rossi J, Berton E, Vigouroux L (2012) Quantification of hand and forearm muscle forces during a maximal power grip task. *Med Sci Sports Exerc* 44:1906–1916
- Gwin JT, Ferris DP (2012) Beta- and gamma-range human lower limb corticomuscular coherence. *Front Hum Neurosci* 6:258
- Hansen NL, Conway BA, Halliday DM, Hansen S, Pyndt HS, Biering-Sorensen F, Nielsen JB (2005) Reduction of common synaptic drive to ankle dorsiflexor motoneurons during walking in patients with spinal cord lesion. *J Neurophysiol* 94:934–942
- Hermens HJ, Freriks B, Disselhorst-Klug C, Rau G (2000) Development of recommendations for SEMG sensors and sensor placement procedures. *J Electromyogr Kinesiol* 10:361–74
- Heroux ME, Gandevia SC (2013) Human muscle fatigue, eccentric damage and coherence in the EMG. *Acta Physiol* 208:294–295
- Hirashima M, Oya T (2016) How does the brain solve muscle redundancy? Filling the gap between optimization and muscle synergy hypotheses. *Neurosci Res* 104:80–87
- Johnston JA, Winges SA, Santello M (2005) Periodic modulation of motor-unit activity in intrinsic hand muscles during multidigit grasping. *J Neurophysiol* 94:206–218
- Kattla S, Lowery MM (2010) Fatigue related changes in electromyographic coherence between synergistic hand muscles. *Exp Brain Res* 202:89–99
- Keenan KG, Collins JD, Massey WV, Walters TJ, Gruszka HD (2011) Coherence between surface electromyograms is influenced by electrode placement in hand muscles. *J Neurosci Methods* 195:10–14
- Kong YK, Hallbeck MS, Jung MC (2010) Crosstalk effect on surface electromyogram of the forearm flexors during a static grip task. *J Electromyogr Kinesiol* 20:1223–1229

- Lee SW, Landers K, Harris-Love ML (2014) Activation and intermuscular coherence of distal arm muscles during proximal muscle contraction. *Exp Brain Res* 232:739–752
- Lemay MA, Crago PE (1999) A dynamic model for simulating movements of the elbow, forearm, and wrist. *J Biomech* 29:1319–1330
- Li ZM, Latash ML, Zatsiorsky VM (1998) Force sharing among fingers as a model of the redundancy problem. *Exp Brain Res* 119:276–286
- Marzke MW, Marchant LF, McGrew WC, Reece SP (2015) Grips and hand movements of chimpanzees during feeding in Mahale Mountains National Park. *Am J Phys Anthropol* 156:317–326
- McClelland VM, Cvetkovic Z, Mills KR (2014) Inconsistent effects of EMG rectification on coherence analysis. *J Physiol* 592: 249–250
- Mima T, Steger J, Schulman AE, Gerloff C, Hallett M (2000) Electroencephalographic measurement of motor cortex control of muscle activity in humans. *Clin Neurophysiol* 111: 326–337
- Mullany H, O'Malley M, St Clair Gibson A, Vaughan C (2002) Agonist–antagonist common drive during fatiguing knee extension efforts using surface electromyography. *J Electromyogr Kinesiol* 12:375–384
- Nazarpour K, Barnard A, Jackson A (2012) Flexible cortical control of task-specific muscle synergies. *J Neurosci* 32:12349–12360
- Norton JA, Gorassini MA (2006) Changes in cortically related intermuscular coherence accompanying improvements in locomotor skills in incomplete spinal cord injury. *J Neurophysiol* 95:2580–2589
- Pizzamiglio S, De Lillo M, Naeem U, Abdalla H, Turner DL (2017) High-frequency intermuscular coherence between arm muscles during robot-mediated motor adaptation. *Front Physiol* 7:668
- Poston B, Danna-Dos Santos A, Jesunathadas M, Hamm TM, Santello M (2010) Force-independent distribution of correlated neural inputs to hand muscles during three-digit Graspin. *J Neurophysiol* 104:1141–1154
- Power HA, Norton JA, Porter CL, Doyle Z, Hui I, Chan KM (2006) Transcranial direct current stimulation of the primary motor cortex affects cortical drive to human musculature as assessed by intermuscular coherence. *J Physiol* 577:795–803
- Semmler JG, Kornatz KW, Enoka RM (2003) Motor-unit coherence during isometric contractions is greater in a hand muscle of older adults. *J Neurophysiol* 90:1346–1349
- Siemionow V, Yao W, Sahgal V, Yue GH, Yang Q (2010) Single-trial EEG-EMG coherence analysis reveals muscle fatigue-related progressive alterations in corticomuscular coupling. *IEEE Trans Neural Syst Rehabil Eng* 18:97–106
- Snijders CJ, Volkers AC, Melchelse K, Vleeming A (1987) Provocation of epicondylalgia lateralis (tennis elbow) by comparing power grip and pinching. *Med Sci Sports Exc* 19:518–523
- Valero-Cuevas FJ, Venkadesan M, Todorov E (2009) Structured variability of muscle activations supports the minimal intervention principle of motor control. *J Neurophysiol* 102:59–68
- Vigouroux L, Domalain M, Berton E (2011) Effect of object width on muscle and joint forces during thumb–index finger graspin. *J Appl Biomech* 27:173–180
- Vigouroux L, Goislard de Monsabert B, Berton E (2015) Estimation of hand and wrist muscle capacities in rock climbers. *Eur J App Physiol* 115:947–957
- von Tscharnner V, Barandun M, Stirling LM (2011) Piper rhythm of the electromyograms of the abductor pollicis brevis muscle during isometric contractions. *J Electromyogr Kinesiol* 21:184–189
- Vrána J, Poláček H, Stančák A (2005) Somatosensory-evoked potentials are influenced differently by isometric muscle contraction of stimulated and non-stimulated hand in humans. *Neurosci Lett* 386:170–175
- Winges SA, Johnston JA, Santello M (2006) Muscle-pair specific distribution and grip-type modulation of neural common input to extrinsic digit flexors. *J Neurophysiol* 96:1258–1266
- Winges SA, Kornatz KW, Santello M (2008) Common input to motor units of intrinsic and extrinsic hand muscles during two-digit object hold. *J Neurophysiol* 99:1119–1126
- Witte M, Patino L, Andrykiewicz A, Hepp-Reymond MC, Kristeva R (2007) Modulation of human corticomuscular beta-range coherence with low-level static forces. *Eur J Neurosci* 26:3564–3570